

## DESIGN, FABRICATION AND ELECTROMECHANICAL CHARACTERISTICS OF A MEMS BASED MICROMIRROR

Talari Rambabu<sup>1</sup>, Mita Dutta<sup>2</sup>

Electrical Engineering Department, Jadavpur University, Kolkata – 700 032, India,  
<sup>1</sup>rambabu\_talari@yahoo.co.in , <sup>2</sup>mita\_dutta@hotmail.com

**Abstract** – In this paper the design, fabrication and electromechanical characteristics of a electrostatic torsional micromirror is presented. In addition to that the static characteristics of a micro-mirror based on the parallel-plate capacitor model are described.

**Keywords:** MEMS, Micro-mirror; Snap-down;

### 1. INTRODUCTION

Micro-mirrors are one of the most important elements in many MEMS (micro-electro-mechanical system) based devices and systems and can be found today in a large variety of applications. Based on their motion types, micro-mirrors can be roughly classified into several groups [1,2] deformable micro mirrors and movable (piston and torsional) micro-mirrors. The deformable micro-mirror is based on the control of the mirror curvature whereas movable mirrors are able to move or rotate in space. Piston micro-mirrors usually move in the direction perpendicular to the mirror plane while torsional mirrors typically rotate about one or two axes.

However, due to their fast response, ease of control, reduced possibility of adhesion, and large array capability, it is the torsional micro-mirrors that dominate the field. These mirrors have been used extensively in digital projection displays, spatial light modulators, optical switches and adaptive optics. Micro-mirrors can be actuated by conventional methods (thermal, pneumatic, magnetic ),as well as by methods that are not normally effective outside the micro scale (electrostatic and piezoelectric ).

Of these methods, electrostatic is a preferred method when small size, low cost, low power and fast response times are necessary. Here we report on the design, fabrication, modeling and static characteristics of a electrostatically actuated, MEMS micro-mirror which meets the requirements of size, angular rotation, actuation voltage.

### 2. OPERATION PRINCIPLE AND ELECTROMECHANICAL MODELING

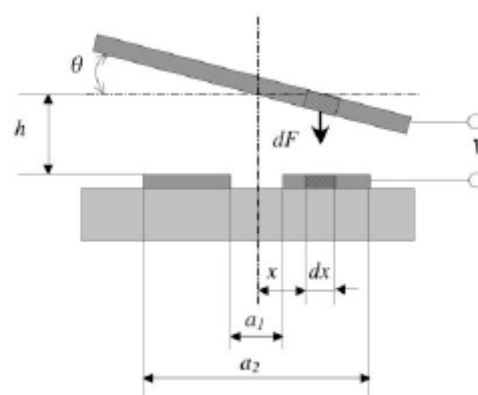


Fig.1. Micro-mirror cross sectional view

Fig.1 shows the cross-sectional view of the proposed micro-mirror. The micro-mirror is supported by two silicon rectangular torsion bars. Further these torsion beams are supported by silicon posts. Two electrodes are placed beneath the mirror. The mirror itself forms the third electrode. A voltage differential between the mirror and lower electrode produces a electrostatic field in the air gap. This field exerts a force on the mirror and produces the actuation. Hence the mirror is tilted around the torsion bars. The mirror can be rotated in another direction by applying potential between other electrode and the mirror. The mechanical restoring torque of the torsion bars restricts the angular moment of the mirror. equilibrium is obtained when the mechanical restoring torque is equal to the electrostatic torque. When a voltage  $V$  is added between the micromirror and one electrode, the electrostatic attraction causes the micromirror to rotate to a certain angle  $\theta$ . In the parallel-plate capacitor model, the micromirror and the electrode are regarded as being composed of an infinite number of infinitesimally-small capacitors of width  $dx$ . Therefore, the electrostatic torque  $M_e$  [1] is given by

$$M_e = \int_{\frac{\beta a}{2}}^{\frac{\alpha a}{2}} x dF = \int_{\frac{\beta a}{2}}^{\frac{\alpha a}{2}} x \frac{\epsilon V^2}{2(h - x \sin \theta)} L dx$$

$$= \frac{\epsilon V^2}{2\theta_{max}^2} L \left[ \frac{1}{1-\beta\phi} - \frac{1}{1-\alpha\phi} \ln \left( \frac{1-\beta\phi}{1-\alpha\phi} \right) \right] \quad (1)$$

Here L and a represent the length and width of the micro-mirror, respectively. And also  $a_1 = \alpha a$ ,  $a_2 = \beta a$ , and  $\phi = \frac{\theta}{\theta_{max}}$  Where  $\theta_{max} = \frac{2h}{a}$  represents the maximum rotation angle.

Hence the electrostatic torque is very sensitive to applied voltage. When the micro-mirror is driven to rotate by electrostatic torque, the angular displacement of the torsion beams will generate an elastic recovery torque. Therefore, the micro-mirror becomes steady only when these torques are balanced (i.e. at the static equilibrium condition).

The elastic recovery torque  $M_r$  that is generated by the torsion beam can be expressed as

$$M_r = S_0 \phi \quad (2)$$

where  $S_0$  denotes the stiffness of the torsion beams. At equilibrium,

$$M_e = M_r \quad (3)$$

Solving the Eq-3 for voltage V

$$V = K_0 \left\{ \frac{\phi^3}{\left[ \frac{1}{1-\beta\phi} - \frac{1}{1-\alpha\phi} \right] + \ln \left[ \frac{1-\beta\phi}{1-\alpha\phi} \right]} \right\}^{1/2} \quad (4)$$

where

$$K_0 = \left[ \frac{2S_0\theta_{max}^3}{\epsilon L} \right]^{1/2}$$

Therefore, the V- $\phi$  relation is mainly determined by the normalized electrode parameters (represented by  $\alpha$  and  $\beta$ ) are involved. From this point of view, it can be said that the electrodes determine the behavior of a torsional micro-mirror.

#### Study of the snap-down effect:

As the driving voltage increases the rotation angle increases gradually upto a point after that the rotation is almost instantaneous. This rotation angle is called snap-down angle. The normalized snap down angle  $\phi_0$  can be obtained theoretically by solving  $\frac{dV}{d\phi} = 0$ . Thus the relation between the normalized snap-down angle  $\phi_0$  and the electrodes parameters  $\alpha$  and  $\beta$  is governed by

$$\beta\phi_0 = 0.4404 \quad (5)$$

Substituting eq-5 in eq-4 the maximum driving voltage is obtained as

$$V_{max} = 0.6432 K_0 \beta^{-3/2} \quad (6)$$

### 3. FABRICATION OF MICROMIRROR

#### 3.1 Finite Element Analysis of micromirror

Finite element analysis (FEA) of micromirror requires the construction of three dimensional structure of micromirror. This 3-D structure can be built by using IntelliSuite's 3D Builder module. This device comprises of four structural layers. The first layer consists of electrodes, the second layer consists of support posts, the third layer consists of support beams, and the fourth layer consists of the mirror body. Mirror segment and electrodes are separated by air gap provided by the posts.

The voltage applied between the mirror segment and the electrodes produces the actuation hence the mirror is displaced through an angle defined by the applied voltage. The four structural layers are constructed in four different levels. Each level height represents the thickness of the corresponding structural layer while fabricating the device. In the first level electrode geometries are drawn, posts are drawn in the second level. In the third level geometry of the support beams is constructed. Mirror segment is drawn in the fourth level. After completion of the drawing, the device appears as shown in the Fig 2.

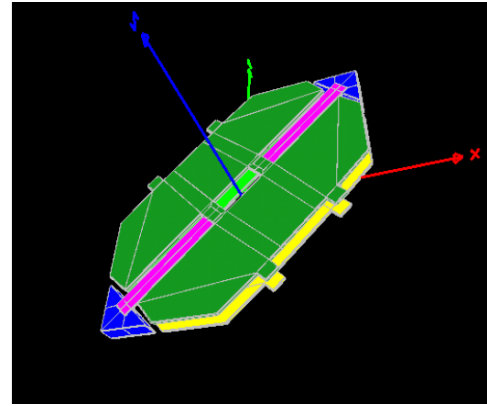


Fig 2. Electrostatically actuated micro-mirror

#### 3.2 Micro-mirror Fabrication

Micro-mirrors have been fabricated with a process that combines the benefits of both bulk and surface-micromachining. Electrostatically actuated micromirror comprises of four structural layers. The first layer consists of electrodes, the second layer consists of support posts, the third layer consists of support beams, and the fourth layer consists of the mirror body. Virtual fabrication of the above device is done by using INTELLISUITE [3] software. The process table for the fabrication of the micro-mirror is presented below. The masks for the fabrication are created in INTELLIMASK. Fig. 3 shows our proposed MEMS micro-mirror with normalized electrode size  $\beta = 0.5$ .

**Process table:**

1. Definition Si Czochralski 100
2. Etch Si Clean Piranha
3. Deposition Al Sputter Ar-Ambi...
4. Definition UV Contact Suss
5. Etch Si Wet Sacrifice
6. Deposition PR-S1800 Spin S1...
7. Etch PR-S1800 Wet 1112A
8. Deposition Si PECVD Generic
9. Definition UV Contact Suss
10. Etch Si Wet KOH
11. Deposition PR-S1800 Spin S...
12. Etch PR-S1800 Wet 1112A
13. Deposition Si PECVD Generic
14. Definition UV Contact Suss
15. Etch Si Wet KOH
16. Etch PR-S1800 Wet 1165
17. Definition UV Contact Suss
18. Etch Al Wet PAN

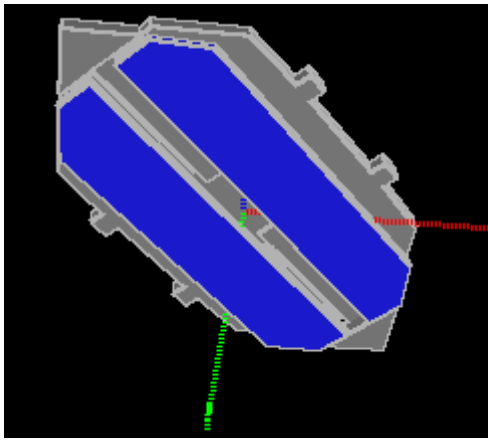


Fig. 3. Proposed MEMS micro-mirror ( $\beta=0.8$ )

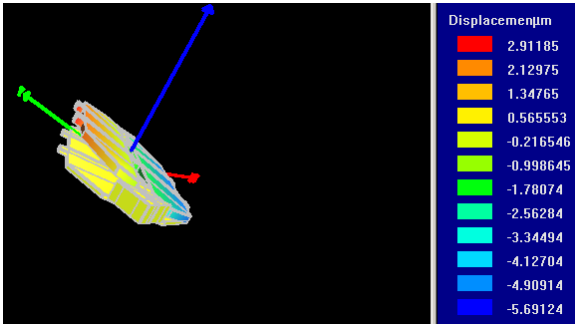


Fig. 4. Micro-mirror at maximum displacement ( $\beta=1$ )

**4. RESULTS**

If the voltage applied to electrodes is varied then the displacement of the micro-mirror changes. Fig .5 shows maximum displacement of the micro-mirror. The angular displacement( $\theta$ ) can be plotted against applied voltage(V) and is shown in fig.5. Initially, the required driving voltage increases with rotation angle. However, when the rotation angle reaches a certain value  $\theta_0$  , the required driving voltage reaches its maximum  $V_{max}$ . This turning point in the curve and the angle are referred to as snap-down point and

snap-down angle ( $\theta_0$ ) respectively. Thereafter, a smaller voltage is required to maintain the torque equilibrium for positions of larger rotation angle. In fact, this kind of balance is not stable and cannot be maintained. When the micro-mirror rotates beyond  $\theta_0$  , it will rapidly snap-down until its edge touches the substrate. This is the well-known snap-down phenomenon. As a result, after the snap-down point, the V- $\theta$  relation will not follow the curve defined by the eq-4. Since the snap-down angle  $\theta_0$  determines the angular range over which the micro-mirror can be smoothly driven, it is an important parameter in applications where the micro-mirror operates in continuous angles (i.e. analog mode), for example, in a laser scanner. Moreover, small snap-down angles can reduce the response time for applications in which torsional micromirror works at on/off states (i.e. digital mode), such as digital projection displays. The maximum driving voltage  $V_{max}$  is also another important parameter in considering practical usage. Equation(6) is plotted and shown in fig.5. Fig.5 shows that the maximum driving voltage( $V_{max}$ ) can be reduced by decreasing the electrode width( $\beta$ ). Similarly, equation(7) is plotted as shown in fig.6 and this depicts that the snap-down angle can be varied by changing  $\beta$ .

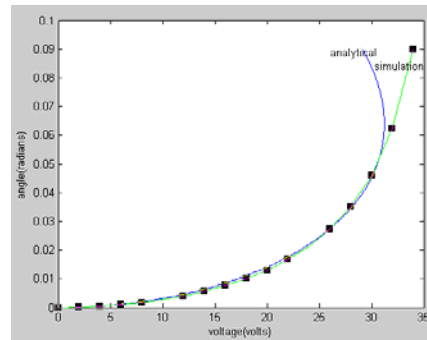


Fig. 5. Angular displacement ( $\theta$ ) vs applied voltage(v)

It is found From fig.5 that the snap-down angle is 0.054 rad ( $3.09^\circ$ ) at approximately 33 volts.

**4.1 Effect of variation of normalized electrode width( $\beta$ ) and voltage at snap-down( $V_{max}$ ) on normalized snap-down angle( $\Phi_0$ )**

Variation in normalized snap-down angle( $\Phi_0$ ) with the variation in the normalized electrode width( $\beta$ )shown in the Fig 6 and from this curve it is observed that as the normalized electrode width( $\beta$ ) increases the normalised rotation angle( $\Phi_0$ ) decreases.

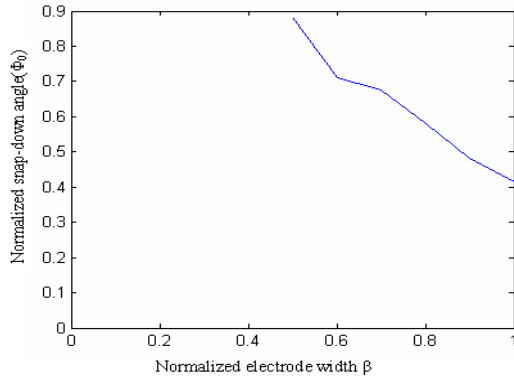


Fig.6. Normalized snap-down angle( $\Phi_0$ ) vs normalized electrode width( $\beta$ )

The voltage at snap-down ( $V_{max}$ ) also varies with the variation in normalized electrode width( $\beta$ ). This variation is plotted in Fig.7. The snap-down voltage decreases with increase in normalized electrode width.

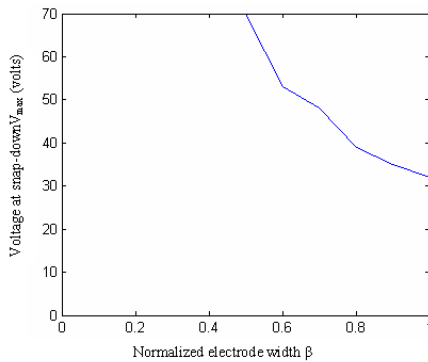


Fig.7. Voltage at snap-down( $V_{max}$ ) vs normalized electrode width( $\beta$ )

#### 4.2 Effect of variation of $\alpha$ and $\beta$ on normalized rotation angle( $\Phi_0$ )

For a particular value of  $\alpha$ , as  $\beta$  varies the normalized rotation angle varies. For different values of  $\alpha$  different values of normalized snap-down angles are obtained. These results are plotted in the Fig.8. For lower values of  $\alpha$  (less than 0.2) the curves between  $\beta$  and  $\Phi_0$  are identical. For values of  $\alpha$  greater than 0.2 the curves lie below. That is as  $\alpha$  value increases the normalized snap-down angle( $\Phi_0$ ) decreases. In other words as the values of  $\alpha$  increase snap-down occurs at small rotation angles.

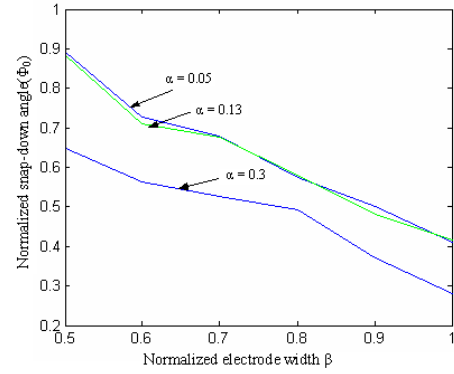


Fig.8. Effect of variation of ' $\alpha$ ' and ' $\beta$ ' on  $\Phi_0$

#### 4.3 Effect of variation of posts height( $h$ ) on angular displacement

Variation in posts height produces the variation in the air gap between mirror segment and the lower electrodes. If the post height is increased the electrostatic force decreases in the air gap thereby decreasing the angular deflection of micromirror for a particular value of applied voltage. For obtaining large angular deflections the micromirror should have sufficient air gap between the mirror segment and the lower electrodes. This increases the voltage required for producing the required angular deflection. These variations are plotted as shown in Fig. 9.

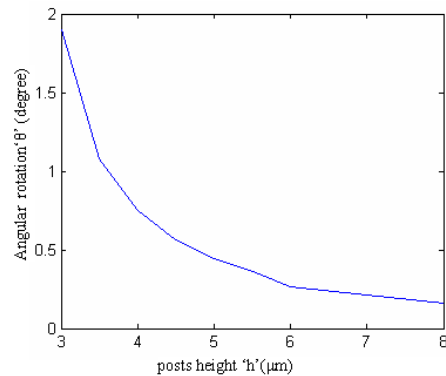


Fig.9. Angular rotation Vs posts height

## 5. CONCLUSION

MEMS based micro-mirror has been modeled and fabricated. The electro-mechanical characteristics of the same under static condition has analyzed. Based on this analysis, the snap-down effect has been investigated and the analytical equations (equ. (5)&(6)) representing the relationships of electrode size with snap-down angle and maximum driving voltage have been obtained. The results obtained through simulation are agreed well with the analytical results.

## REFERENCES

- [1]. X.M. Zhanga, F.S. Chaub, C. Quanb, Y.L. Lama, A.Q. Liua , “ Study of the static characteristics of a torsional micro-mirror”, Sens. Actuators Elsevier Journal, vol. A90 , pp. 73-81 , 2001.
- [2]. Slava Krylov and Daniel I Barnea , “ Bouncing mode electrostatically actuated scanning micro-mirror for video applications” , Smart Mater. Struct. Vol. 14 , pp.1281–1296 ,2005.
- [3]. INTELLISUITE user manual ,version-8.1,page No.92-115.